Eggshell Biowaste-Derived Flexible and Self-Cleaning Films for Efficient Subambient Daytime Radiative Cooling

Shiwen Wu, Ruda Jian, Lyu Zhou, Siyu Tian, Tengfei Luo, Shuang Cui, Bo Zhao, and Guoping Xiong*

Cite This: ACS Appl. Mater. Interfaces 2023, 15, 44820−44826   Read Online

ACCESS | � Metrics & More | 📖 Article Recommendations | SI Supporting Information

ABSTRACT: The management of the abundant eggshell biowaste produced worldwide has become a problematic issue due to the generated odor and microorganisms after direct disposal of the eggshell biowaste in landfills. Herein, we propose a new method to convert the hazardous eggshell biowaste to valuable resources for energy management applications. Eggshell-based films are fabricated by embedding eggshell powders into a polymer matrix to achieve highly efficient subambient daytime radiative cooling. Benefiting from the Mie scattering of the eggshell particles/ air pores in the solar spectrum and the strong emission of the eggshell in the mid-infrared (mid-IR) range, the eggshell-based films present a high reflection of 0.96 in the solar spectrum and a high emission of 0.95 in the mid-IR range, with notable average temperature reductions of 4.1 and 11 °C below the ambient temperature during daytime and nighttime, respectively. Moreover, the eggshell-based films exhibit excellent flexibility and self-cleaning properties, which are beneficial for practical long-term outdoor applications. Our proposed design provides a new means for environmentally friendly and sustainable management of eggshell biowaste.

KEYWORDS: eggshell biowaste, passive daytime radiative cooling, Mie scattering, flexible, self-cleaning
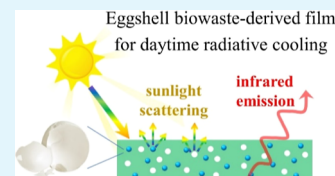
1. INTRODUCTION

Eggs have become one of the most important food resources worldwide because they provide essential nutrients for the human body.[1] In 2020, the annual global egg production reached 8.7×10^7 tons, and this value is still increasing rapidly.[2,3] However, enormous amount of the eggshell is also generated from the daily consumption of eggs and is generally considered as a worthless, hazardous biowaste according to European Union regulations.[4] Most of the eggshell biowaste is commonly abandoned and directly disposed in landfills, resulting in gradual propagation of harmful odor and microorganisms.[5,6] Converting waste to valuable and useful resources has become a mainstreaming trend in the 21st century according to the 3R principles (i.e., reduce, reuse, and recycle) for promoting the circular economy.[7] Therefore, finding an effective route to manage eggshell biowaste in an environmentally friendly and sustainable manner is highly desirable.

Recently, passive daytime radiative cooling has attracted tremendous attention due to its passive nature and potential to operate during the daytime.[8−13] An outer space with an ultralow temperature of approximately 3 K performs as a perfect heat sink for heat transfer processes.[14] The coincident overlapping between the atmospheric transparency window on the earth (i.e., 8−13 μm) and the spectral peak of blackbody radiation at 300 K provides the objects on the earth an efficient way to eliminate heat and thus passively cool down their temperature through thermal radiative emissions into the outer space.[15,16] Given that light absorption within the solar spectrum is minimized simultaneously, passive cooling of the

surfaces below ambient temperature can be achieved even during the daytime without an external energy input.[17] The main component of the eggshell is calcium carbonate ($CaCO_3$), which possesses abundant absorption peaks and thus high emission in the mid-infrared (mid-IR) range.[18,19] Therefore, eggshell biowaste is highly likely to act as an effective component in radiative cooling materials.

Herein, we report the design of eggshell biowaste-derived films with excellent flexibility and self-cleaning functions to achieve subambient daytime radiative cooling. Through optimizing the experimental parameters, the sizes of the eggshell particles and air pores in the polymer matrix are adjusted to a submicron range to efficiently scatter sunlight by Mie scattering. Meanwhile, strong absorption of the eggshell powders originating from the stretching and bending of the C−O and Ca−O bonds provides high emission in the mid-IR range. Consequently, a high reflection of 0.96 in the solar spectrum and a high emission of 0.95 in the mid-IR range are achieved by the eggshell-based films, which are comparable to or even higher than those of the state-of-the-art radiative cooling materials. Outdoor field tests show that average temperature reductions of 4.1 and 11 °C below the ambient temperature during daytime and nighttime can be achieved,
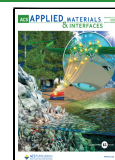
respectively. Moreover, the outstanding flexibility and water-repellent properties enable the eggshell-based films to survive complex outdoor conditions without deteriorating their radiative cooling performance. Our design provides an effective way to convert eggshell biowaste to environmentally friendly functional materials.

2. EXPERIMENTAL SECTION

2.1. Preparation of Eggshell Powders. Eggshells were collected from consumed eggs purchased from local supermarkets. First, 10 g of eggshell was added into 100 mL of 6% H_2O_2 solution and heated at 90 °C for 1 h to remove the impurities. After being rinsed by water several times and dried at 80 °C, the eggshells were broken down to eggshell powders by a vertical planetary ball-mill machine (Biobase Bkbm-V0.4). Zirconium dioxide balls and containers were used in the ball-milling process, and the milling speed was fixed at 700 rpm for 24 h.

2.2. Preparation of Eggshell-Based Polymethylpentene Films. 5.4 g of ball-milled eggshell powders and 1.2 mL of KH550 (Sigma-Aldrich) were added to 40 mL of cyclohexane (Sigma-Aldrich) to prepare eggshell/cyclohexane suspensions. Then, 2.23 g of polymethylpentene (TPX) (Sigma-Aldrich) was added and dissolved in the cyclohexane solvent at 65 °C. Subsequently, the prepared eggshell/TPX solutions were poured into a tap-casting mold and frozen at −60 °C. The E-TPX films were obtained after a freeze-drying process for 48 h. For comparison, porous TPX films were fabricated by the same procedure without incorporating the eggshell powders, and the TPX films devoid of air pores were fabricated by naturally drying TPX solution on a Teflon sheet.

2.3. Characterization. Reflectivity spectra in the solar spectrum and emissivity spectra in the mid-IR range were measured by a UV−vis NIR spectrometer (Agilent Cary 5000) and a Bruker VERTEX 70 FTIR equipped with integrating spheres, respectively. The Fourier transform infrared (FTIR) spectra of the eggshell powders were recorded using an FTIR spectrometer (Agilent 660-2). The morphology and microstructures of the samples were characterized using a field-emission scanning electron microscope (Supra 40, Zeiss).

2.4. Numerical Simulations. The optical properties of the air pores and eggshell particles were simulated by commercial finite-difference time-domain (FDTD) software (Lumerical 2023). In the simulations, the total-field scattered-field source was employed to investigate the light scattering effects of the air pores and eggshell particles. Perfectly matching layer boundary conditions were adopted in all directions, and a mesh size of 10 nm was applied. Theoretical calculations were also conducted by Lorenz−Mie theory[20] to validate the FDTD simulation results.

2.5. Outdoor Radiative Cooling Performance Measurements. The outdoor radiative cooling field tests were conducted on sunny days in Richardson (96.73°W, 32.95°N, Texas, U.S.). An all-in-one weather sensor (WS 500, Lufft) was placed beside the experimental setup to measure the weather conditions, including ambient temperature, relative humidity, and wind speed. The solar irradiance was recorded by a pyranometer (CMP 3, Kipp & Zonen). Both the weather sensor and the pyranometer were connected to a datalogger (XLink 500, SUTRON) for data collection.

3. RESULTS AND DISCUSSION

Figure 1 schematically shows the fabrication process of the E-TPX films. Here, TPX is employed as the polymer matrix because of its excellent transmittance in both solar spectrum and IR range.[21−24] Briefly, the ground eggshell powders were initially dispersed in cyclohexane, and then, TPX was added and dissolved into the cyclohexane solvents to obtain the eggshell/TPX solutions. The amount of eggshell powders and TPX was optimized to achieve efficient passive daytime radiative cooling (details shown in Supporting Information
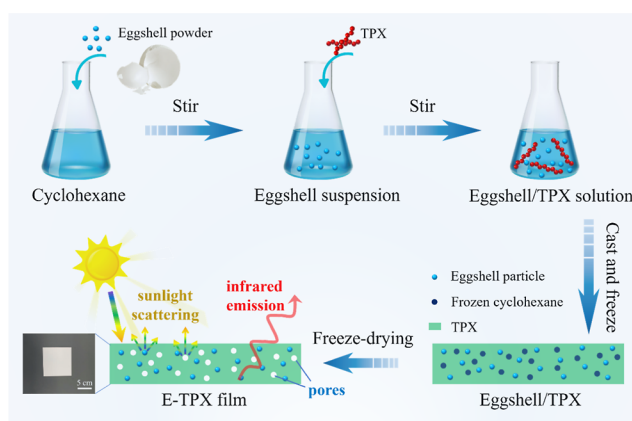

Figure 1. Schematic showing the fabrication process of the E-TPX films.

Section S1). Subsequently, the eggshell/TPX solution was tape-cast with a fixed thickness of 600 μm and frozen at −60 °C. After the sublimation of the frozen cyclohexane solvent during the freeze-drying process, the E-TPX films containing a large amount of embedded air pores and eggshell particles were obtained.

The E-TPX film exhibits an outstanding mechanical performance. As shown in Figure 2a, an E-TPX film with a width of 1 cm can hold up to 500 g of weight. Moreover, the free-standing E-TPX film can be easily recovered to the original shape after being twisted, bent, or curved to a spiral shape (Figure 2b), demonstrating its excellent flexibility, which is highly desirable to cool surfaces with complex structures for wider applications. Figure 2c presents the cross-sectional SEM images of the E-TPX films at different magnifications. The eggshell particles with diameters around hundreds of nanometers are uniformly distributed in the TPX matrix, which can be further indicated by the energy-dispersive X-ray analysis (EDAX) mapping of the E-TPX film shown in Figure 2d. In addition, abundant air pores can also be observed in the TPX networks, with the size optimized to a submicron range by adjusting the ratio of TPX to cyclohexane in the fabrication process (Supporting Information Figure S1).

The sizes of the air pores and eggshell particles in the E-TPX film are measured and collected by open software, ImageJ. As shown in Figure 3a, the air pores and eggshell particles are dispersed in the E-TPX film with broad distributions centered at 0.42 and 0.75 μm, respectively. Figure 3b presents the simulated scattering cross-sectional spectra of the air pores in the TPX matrix with several typical sizes chosen from Figure 3a. Benefiting from the collective effects of multiple geometric sizes, the air pores can effectively scatter light in the wavelength range of ~0.3−1 μm. The optical properties of the main component of the eggshell,[25] $CaCO_3$, are adopted in the FDTD simulations to investigate the light scattering effect of the eggshell particles. As shown in Figure 3c, the eggshell particles embedded in the E-TPX film strongly scatter light in the wavelength range of ~0.5−1.6 μm. Both FDTD simulation results of the air pores and eggshell particles agree well with the results calculated by Lorenz−Mie theory[20] (Supporting Information Figure S3). Therefore, the eggshell particles and air pores concurrently improve light scattering in the wavelength ranges where solar irradiance is intense due to Mie scattering,[26] leading to an overall high reflection in the solar spectrum.
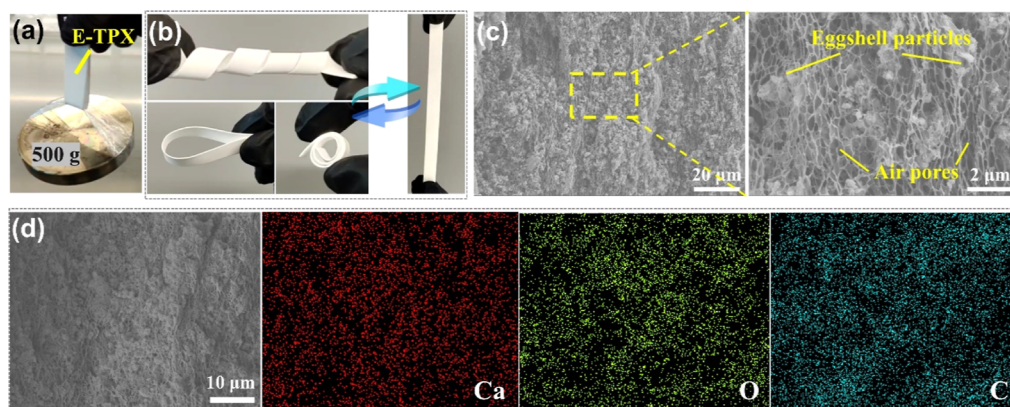
Figure 2. (a) Photograph showing that an E-TPX film with a 1 cm width can hold 500 g of weight. (b) Photographs showing that the E-TPX film can be recovered to the original shape after being twisted, bent, or curved to a spiral shape. (c) Cross-sectional SEM images of the E-TPX films. (d) EDAX mapping of the E-TPX film showing the elemental distributions of Ca, O, and C.
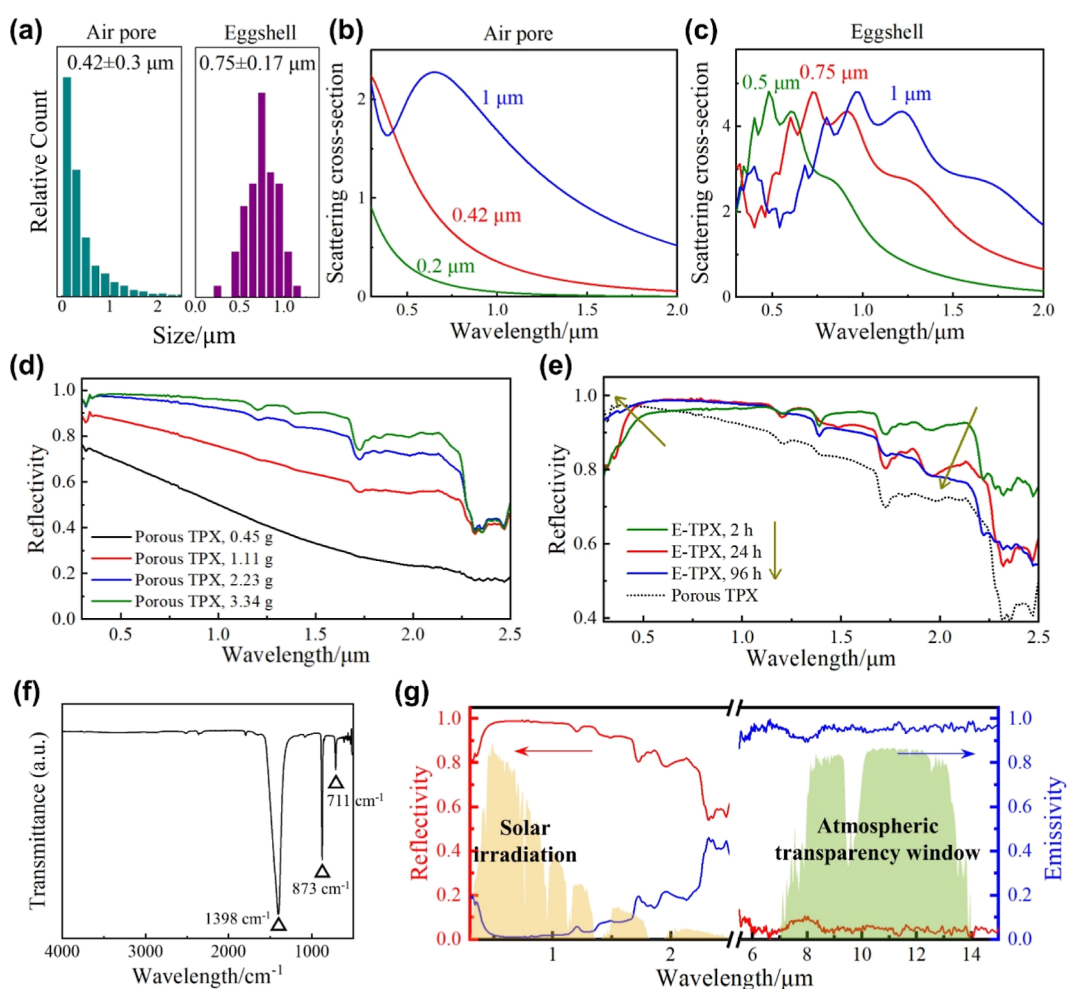

Figure 3. (a) Size distributions of the air pores and eggshell particles in the E-TPX film, with the number-weighted mean pore size calculated to be 0.42 and 0.75 μm, respectively. (b) Simulated scattering cross-sectional spectra of the air pores with sizes of 0.2, 0.42, and 1 μm. (c) Simulated scattering cross-sectional spectra of the eggshell particles with sizes of 0.5, 0.75, and 1 μm. (d) Reflectivity spectra of the porous TPX films fabricated by dissolving different amounts of TPX in 40 mL of cyclohexane. (e) Reflectivity spectra of the E-TPX films fabricated by introducing eggshell particles ball-milled for different durations. The dashed line represents the porous TPX film in the absence of the eggshell particles. (f) FTIR spectrum of the eggshell powders. (g) Reflectivity and emissivity spectra of the E-TPX films in the solar spectrum and mid-IR regime.

We further adjusted the fabrication parameters to investigate the influence of the sizes of air pores and eggshell particles on the optical properties in the solar spectrum. First, the porous TPX films with different ratios of TPX/cyclohexane are produced. With an increase in the quantity of the dissolved TPX, a greater number of submicron air pores are formed (Supporting Information Figure S1), leading to enhanced solar reflection (Figure 3d). Note that excessive TPX concentration

leads to increased viscosity in the eggshell/TPX solution, hindering the uniform dispersion of the eggshell particles. Therefore, the amount of dissolved TPX is maintained as 2.23 g in 40 mL of cyclohexane for the fabrication of the E-TPX films. Subsequently, the E-TPX films with different eggshell particle sizes are fabricated by incorporating the eggshell particles subjected to distinct ball-milling durations. The size of the eggshell particle diminishes as the ball-milling duration extends (Supporting Information Figure S2). As shown in Figure 3e, the E-TPX films produced through a 2 h ball-milling process exhibit higher reflectivity in the near-IR range but comparatively diminished reflectivity in the ultraviolet (UV) and visible regions. Conversely, with an increase in the ball-milling duration to 96 h, reflectivity is enhanced in the UV and visible regions but drops significantly in the near-IR range. Such an observation agrees well with our simulation results, which indicate that a reduction in the eggshell particle size leads to a blueshift of the reflectivity peak (Figure 3c). In the following analysis, we fixed the ball-milling duration of the eggshells at 24 h to fabricate the E-TPX films. Additionally, the content of the eggshell particles can affect the optical properties of the E-TPX films (Supporting Information Section S1).

Meanwhile, the chemical structures of the eggshell powders are characterized by FTIR and are shown in Figure 3f. The FTIR spectrum of the eggshell powders exhibits strong absorption peaks in the mid-IR range. The peaks at 1398 and 873 cm^{-1} correspond to the C−O stretching and bending of the main component, $CaCO_3$, in eggshell powders, respectively, while the sharp peak at 710 cm^{-1} represents the Ca−O bond.[19] These absorption peaks of the eggshell powders enable a strong emission of the E-TPX films in the mid-IR range. Consequently, the E-TPX films exhibit exceptional optical properties with a weighted average reflection of 96% in the solar spectrum and an emission of 95% in the mid-IR range (Figure 3g), which are comparable to or even higher than those of the state-of-the-art passive daytime radiative cooling materials (Supporting Information Table S1).[10,11,27−32]

The radiative cooling performance of the E-TPX films was evaluated in outdoor field tests. Figure 4a,b presents our customized experimental setup for radiative cooling field tests. The radiative cooling samples were placed on the top of a highly insulating vacuum insulation panel [(VIP), with a thermal conductivity of ~2 mW m^{-1} K^{-1}], sitting inside an expanded polystyrene foam [(EPS), with a thermal conductivity of ~30−40 mW m^{-1} K^{-1}] box to minimize the parasitic heat gains to the back side of the samples. The EPS box was further covered by a 10 μm thick polyethylene film to reduce convective heat loss and improve thermal isolation. A k-type thermocouple was placed underneath the testing films to measure the real-time temperatures of the testing samples. The outdoor field test spanned a continuous 24 h period on a sunny summer day in Richardson (96.73°W, 32.95°N, Texas, U.S.). An image of the entire outdoor test system is shown in Supporting Information Figure S6. The real-time solar irradiance and relative humidity were measured and are shown in Figure 4c,d, and the wind speed during the test was around 1−4 m s^{-1} (Supporting Information Figure S7). Benefiting from the high solar reflection and high infrared emission, a significant subambient cooling effect was achieved by the E-TPX films during the 24 h test period (Figure 4e). During the midday hours (12:00−14:00), under a solar irradiance of up to 983.7 W m^{-2}, the E-TPX films exhibited an
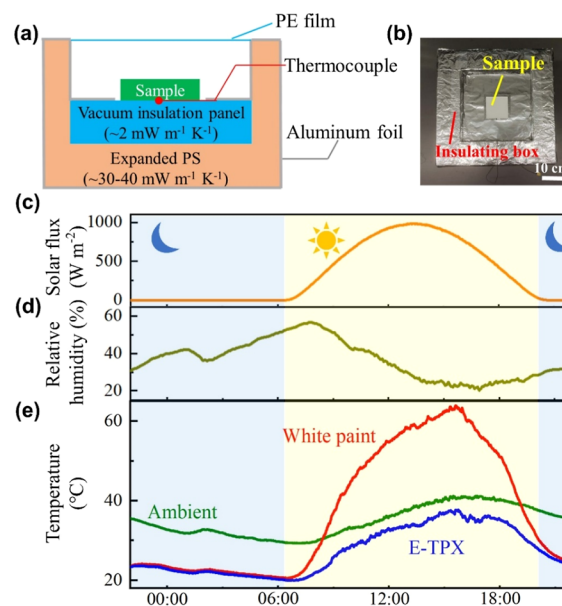

Figure 4. (a) Schematic and (b) photograph of our experimental setup for radiative cooling field tests. (c) Solar irradiance, (d) relative humidity, and (e) measured temperatures of the ambient, white paint, and the E-TPX film as functions of time when exposed on sunny days in Richardson, Texas, U.S. during the outdoor field test from 22:00, July 17, 2023 to 22:00, July 18, 2023.

average temperature reduction of 4.1 °C compared to the ambient temperature. In comparison, the temperature of white paint rose to 21 °C higher than the ambient temperature. Moreover, the E-TPX films exhibited a subambient cooling of 11 °C during the nighttime. Another outdoor field test was performed in Reno (119.81°W, 39.53°N, Nevada, U.S.) with a completely different weather condition, where an average temperature drop of 6 and 13 °C below the ambient temperature around noon and during nighttime were observed (Supporting Information Figure S8), respectively, indicating the outstanding subambient radiative cooling capability of the E-TPX films.

Following a reported procedure in a prior work,[13,17] we employed a heater positioned at the backside of the E-TPX film to experimentally quantify the cooling power density of the film. To ensure uniform heating, a 100 μm thick copper sheet was sandwiched between the E-TPX film and the heater. The heater was connected to a power supply (Stonylab), offering adjustable power to elevate the temperature of the E-TPX film to match that of the ambient environment. Consequently, the local cooling power density of the E-TPX film can be measured, which is equal to the applied heating power under this steady-state condition. Daytime cooling power measurement was conducted on a sunny day with an average solar irradiance of 941.1 W m^{-2} (Figure 5a). We manually modulated the heating power (Figure 5b) until the temperature of the E-TPX film reached equilibrium with the ambient temperature (Figure 5c). As a result, the daytime cooling power density of the E-TPX film was determined to be 66.3 W m^{-2}. Likewise, the nighttime cooling power density of the E-TPX film was measured to be 117.4 W m^{-2} (Figure 5d−f).

The surfaces of the radiative cooling materials inevitably suffer from rain flushing and dust contamination when exposed to outdoor environments, which may result in severe
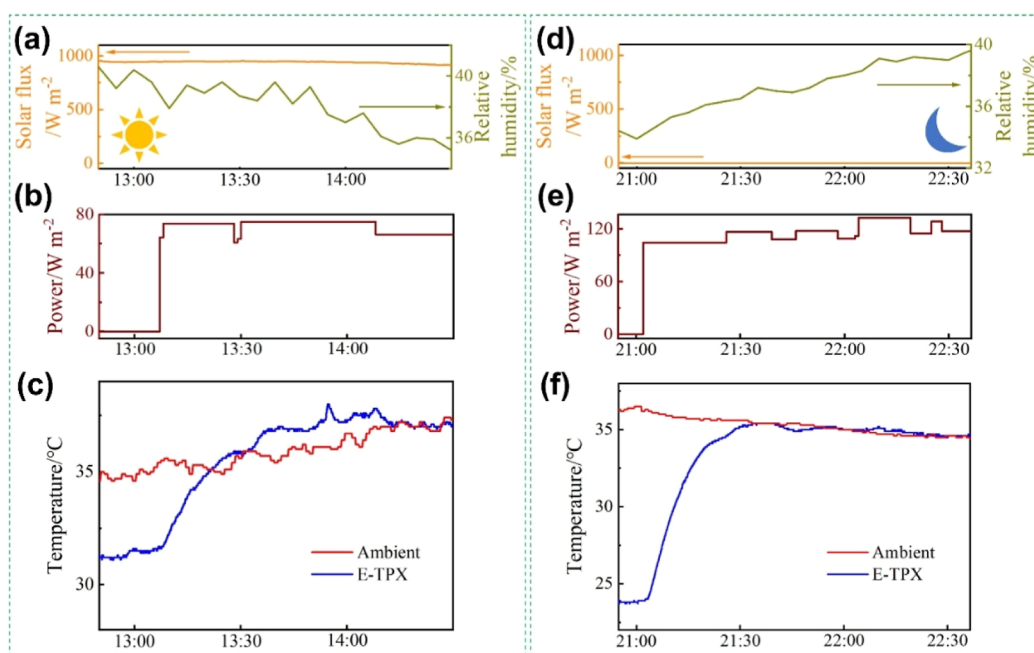
Figure 5. (a) Weather conditions, (b) measured heater power, and (c) temperatures of the E-TPX film and the ambient environment during the daytime cooling power measurement. (d) Weather conditions, (e) measured heater power, and (f) temperatures of the E-TPX film and the ambient environment during the nighttime cooling power measurement.
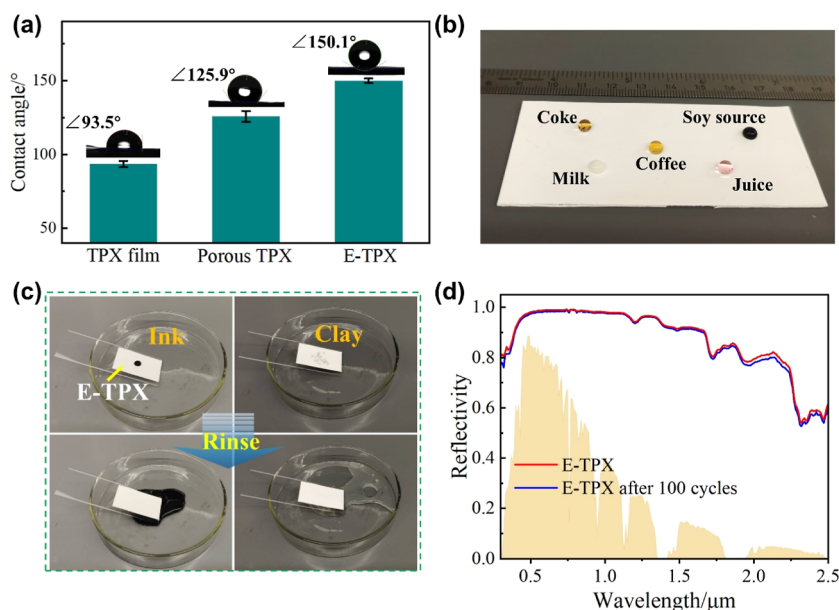

Figure 6. (a) Water contact angles on the TPX, porous TPX, and E-TPX films. (b) Photograph showing the droplets of coke, milk, coffee, soy sauce, and juice placed on the E-TPX film. (c) Photographs showing the self-cleaning capability of the E-TPX films. Ink and clay can be easily removed from the E-TPX film by water rinsing. (d) Reflectivity spectra of the E-TPX film before and after 100 cycles of ink contamination and water rinsing.

deterioration of the cooling performance. The surface wettabilities of the TPX film, porous TPX film, and E-TPX film are characterized. As shown in Figure 6a, the introduction of the air pores into the TPX film results in an increase in the water contact angle from 93.5 to 125.9°, and further adding eggshell particles leads to an enhancement to 150.1°. These findings suggest that the superhydrophobic performance of the E-TPX film can be ascribed to the increased surface roughness arising from the existence of the air pores and eggshell particles.[11,33] Moreover, the water contact angle can also be

affected by the contents of the air pores and eggshell particles (Supporting Information Figures S9 and S10). The E-TPX films can also repel a wide range of possible liquid contaminants (e.g., coke, milk, coffee, soy sauce, and juice) in daily life (Figure 6b). The superhydrophobicity and liquid-repellent properties protect the E-TPX films from being damaged by rain and liquid contaminants. Moreover, the self-cleaning performance of the E-TPX films is also demonstrated, as shown in Figure 6c. Ink droplets and clay were placed on the surface of the E-TPX film as representatives of liquid and solid

contaminants, respectively. These contaminants can be easily removed from the E-TPX film by rinsing with water droplets. Notably, after up to 100 cycles of ink contamination on the surface of the E-TPX film and subsequent water rinsing, the reflectivity of the E-TPX film exhibits negligible changes (Figure 6d). In this manner, the E-TPX films can repel water and clean dirt contaminations during rainy days, indicating its long-term outstanding durability for outdoor applications.

4. CONCLUSIONS

In summary, we report eggshell biowaste-derived films for efficient subambient daytime radiative cooling. The as-prepared E-TPX films exhibit a high reflection of 0.96 in the solar spectrum due to the Mie scattering of the embedded eggshell particles and abundant air pores in the TPX matrix and a high emission of 0.95 in the mid-IR range due to the strong infrared absorption of the eggshell. Consequently, the radiative cooling material achieves subambient cooling effect with average temperature reductions of 4.1 and 11 °C below the ambient temperature during daytime and nighttime, respectively. Moreover, the E-TPX films show excellent flexibility and self-cleaning properties, which are crucial for long-term outdoor applications. The design of the E-TPX films provides a new means for the sustainable and environmentally friendly management of eggshell biowastes.

■ ASSOCIATED CONTENT

ⓈⒾ Supporting Information

The Supporting Information is available free of charge at https://pubs.acs.org/doi/10.1021/acsami.3c06296

> Optimization on experimental parameters; cross-sectional SEM images of the porous TPX films; cross-sectional SEM images of the E-TPX films fabricated by introducing eggshell particles ball-milled for different durations; scattering cross-section spectra of the air pores and eggshell particles calculated by FDTD simulations or Lorenz−Mie theory; reflectivity and emissivity spectra of the E-TPX films with different content of eggshell particles; cross-sectional SEM images of the E-TPX films with different eggshell contents; photo of the setup for outdoor radiative cooling measurement; wind speed as a function of time during the outdoor test; measured temperatures of the ambient environment and the E-TPX film as functions of time in Reno, Nevada, U.S.; water contact angles on the porous TPX films and E-TPX films; and comparison between radiative cooling performance between our proposed eggshell biowaste-derived film and previous devices (PDF)

■ AUTHOR INFORMATION

Corresponding Author

Guoping Xiong − *Department of Mechanical Engineering, The University of Texas at Dallas, Richardson, Texas 75080, United States*; Email: guoping.xiong@utdallas.edu

Authors

Shiwen Wu − *Department of Mechanical Engineering, The University of Texas at Dallas, Richardson, Texas 75080, United States*; ⓞ orcid.org/0000-0001-8065-0684

Ruda Jian − *Department of Mechanical Engineering, The University of Texas at Dallas, Richardson, Texas 75080, United States*

Lyu Zhou − *Department of Mechanical Engineering, The University of Texas at Dallas, Richardson, Texas 75080, United States*

Siyu Tian − *Department of Mechanical Engineering, The University of Texas at Dallas, Richardson, Texas 75080, United States*; ⓞ orcid.org/0000-0001-6463-0691

Tengfei Luo − *Department of Aerospace and Mechanical Engineering, University of Notre Dame, Notre Dame, Indiana 46556, United States*; ⓞ orcid.org/0000-0003-3940-8786

Shuang Cui − *Department of Mechanical Engineering, The University of Texas at Dallas, Richardson, Texas 75080, United States*

Bo Zhao − *Department of Mechanical Engineering, University of Houston, Houston, Texas 77004, United States*

Complete contact information is available at:
https://pubs.acs.org/10.1021/acsami.3c06296

Notes

The authors declare no competing financial interest.

■ ACKNOWLEDGMENTS

■ REFERENCES

(1) Pirvutoiu, I.; Popescu, A. Research on the Major Trends in the Romanian Egg Market. *Bull. Univ. Agric. Sci.* **2012**, *69* (2), 229−238.

(2) Shahbandeh, M. Global egg production from 1990 to 2021. Statista. https://www.statista.com/statistics/263972/egg-production-worldwide-since-1990/ (accessed Jan 25, 2023).

(3) Food and Agriculture Organization of the United Nations. https://www.fao.org/poultry-production-products/production/en/ (accessed 2023-09-04).

(4) Mignardi, S.; Archilletti, L.; Medeghini, L.; De Vito, C. Valorization of Eggshell Biowaste for Sustainable Environmental Remediation. *Sci. Rep.* **2020**, *10* (1), 2436.

(5) Sarder, M. R.; Hafiz, N. A.; Alamgir, M. In Study on the Effective Reuse of Eggshells as a Resource Recovery from Municipal Solid Waste. *Waste Management and Resource Efficiency*; Ghosh, S. K., Ed.; Springer: Singapore, 2019; pp 71−79.

(6) Meng, X.; Deng, D. Trash to Treasure: Waste Eggshells Used as Reactor and Template for Synthesis of Co9S8 Nanorod Arrays on Carbon Fibers for Energy Storage. *Chem. Mater.* **2016**, *28* (11), 3897−3904.

(7) Quina, M. J.; Soares, M. A. R.; Quinta-Ferreira, R. Applications of Industrial Eggshell as a Valuable Anthropogenic Resource. *Resour., Conserv. Recycl.* **2017**, *123*, 176−186.

(8) Zhou, L.; Rada, J.; Zhang, H.; Song, H.; Mirniaharikandi, S.; Ooi, B. S.; Gan, Q. Sustainable and Inexpensive Polydimethylsiloxane Sponges for Daytime Radiative Cooling. *Adv. Sci.* **2021**, *8* (23), 2102502.

(9) Li, T.; Zhai, Y.; He, S.; Gan, W.; Wei, Z.; Heidarinejad, M.; Dalgo, D.; Mi, R.; Zhao, X.; Song, J.; Dai, J.; Chen, C.; Aili, A.; Vellore, A.; Martini, A.; Yang, R.; Srebric, J.; Yin, X.; Hu, L. A Radiative Cooling Structural Material. *Science* **2019**, *364* (6442), 760−763.

(10) Mandal, J.; Fu, Y.; Overvig, A. C.; Jia, M.; Sun, K.; Shi, N. N.; Zhou, H.; Xiao, X.; Yu, N.; Yang, Y. Hierarchically Porous Polymer Coatings for Highly Efficient Passive Daytime Radiative Cooling. *Science* **2018**, *362* (6412), 315−319.

(11) Huang, M.-C.; Xue, C.-H.; Huang, J.; Liu, B.-Y.; Guo, X.-J.; Bai, Z.-X.; Wei, R.-X.; Wang, H.-D.; Du, M.-M.; Jia, S.-T.; Chen, Z.; Lai, Y. A Hierarchically Structured Self-Cleaning Energy-Free Polymer Film for Daytime Radiative Cooling. *Chem. Eng. J.* **2022**, *442*, 136239.

(12) Zhou, L.; Song, H.; Liang, J.; Singer, M.; Zhou, M.; Stegenburgs, E.; Zhang, N.; Xu, C.; Ng, T.; Yu, Z.; Ooi, B.; Gan, Q. A Polydimethylsiloxane-Coated Metal Structure for All-Day Radiative Cooling. *Nat. Sustain.* **2019**, *2* (8), 718−724.

(13) Zhou, L.; Song, H.; Zhang, N.; Rada, J.; Singer, M.; Zhang, H.; Ooi, B. S.; Yu, Z.; Gan, Q. Hybrid Concentrated Radiative Cooling and Solar Heating in a Single System. *Cell Rep. Phys. Sci.* **2021**, *2* (2), 100338.

(14) Zhou, L.; Rada, J.; Tian, Y.; Han, Y.; Lai, Z.; McCabe, M. F.; Gan, Q. Radiative Cooling for Energy Sustainability: Materials, Systems, and Applications. *Phys. Rev. Mater.* **2022**, *6* (9), 090201.

(15) Yin, X.; Yang, R.; Tan, G.; Fan, S. Terrestrial Radiative Cooling: Using the Cold Universe as a Renewable and Sustainable Energy Source. *Science* **2020**, *370* (6518), 786−791.

(16) Zhao, D.; Aili, A.; Zhai, Y.; Xu, S.; Tan, G.; Yin, X.; Yang, R. Radiative Sky Cooling: Fundamental Principles, Materials, and Applications. *Appl. Phys. Rev.* **2019**, *6* (2), 021306.

(17) Raman, A. P.; Anoma, M. A.; Zhu, L.; Rephaeli, E.; Fan, S. Passive Radiative Cooling below Ambient Air Temperature under Direct Sunlight. *Nature* **2014**, *515* (7528), 540−544.

(18) Wu, S.-C.; Tsou, H.-K.; Hsu, H.-C.; Hsu, S.-K.; Liou, S.-P.; Ho, W.-F. A Hydrothermal Synthesis of Eggshell and Fruit Waste Extract to Produce Nanosized Hydroxyapatite. *Ceram. Int.* **2013**, *39* (7), 8183−8188.

(19) Rohim, R.; Ahmad, R.; Ibrahim, N.; Hamidin, N.; Abidin, C. Z. A. Characterization of Calcium Oxide Catalyst from Eggshell Waste. *Adv. Environ. Biol.* **2014**, *8* (22), 35−38.

(20) Bohren, C.; Huffman, D. Absorption and Scattering of Light by Small Particles; *Absorption and Scattering by a Sphere*; John Wiley & Sons, 1998; pp 82−129.

(21) Zhang, R.; Xiang, B.; Shen, Y.; Xia, L.; Xu, L.; Guan, Q.; Tang, S. Energy-Efficient Smart Window Based on a Thermochromic Microgel with Ultrahigh Visible Transparency and Infrared Transmittance Modulation. *J. Mater. Chem. A* **2021**, *9* (32), 17481−17491.

(22) Zhai, Y.; Ma, Y.; David, S. N.; Zhao, D.; Lou, R.; Tan, G.; Yang, R.; Yin, X. Scalable-Manufactured Randomized Glass-Polymer Hybrid Metamaterial for Daytime Radiative Cooling. *Science* **2017**, *355* (6329), 1062−1066.

(23) Feng, J.; Gao, K.; Jiang, Y.; Ulpiani, G.; Krajcic, D.; Paolini, R.; Ranzi, G.; Santamouris, M. Optimization of Random Silica-Polymethylpentene (TPX) Radiative Coolers towards Substantial Cooling Capacity. *Sol. Energy Mater. Sol. Cells* **2022**, *234*, 111419.

(24) Chen, G.; Wang, Y.; Qiu, J.; Cao, J.; Zou, Y.; Wang, S.; Ouyang, J.; Jia, D.; Zhou, Y. A Visibly Transparent Radiative Cooling Film with Self-Cleaning Function Produced by Solution Processing. *J. Mater. Sci. Technol.* **2021**, *90*, 76−84.

(25) Ghosh, G. Dispersion-Equation Coefficients for the Refractive Index and Birefringence of Calcite and Quartz Crystals. *Opt. Commun.* **1999**, *163* (1−3), 95−102.

(26) Cai, L.; Song, A. Y.; Li, W.; Hsu, P.-C.; Lin, D.; Catrysse, P. B.; Liu, Y.; Peng, Y.; Chen, J.; Wang, H.; Xu, J.; Yang, A.; Fan, S.; Cui, Y. Spectrally Selective Nanocomposite Textile for Outdoor Personal Cooling. *Adv. Mater.* **2018**, *30* (35), 1802152.

(27) Liu, X.; Zhang, M.; Hou, Y.; Pan, Y.; Liu, C.; Shen, C. Hierarchically Superhydrophobic Stereo-Complex Poly (Lactic Acid) Aerogel for Daytime Radiative Cooling. *Adv. Funct. Mater.* **2022**, *32* (46), 2207414.

(28) Yao, P.; Chen, Z.; Liu, T.; Liao, X.; Yang, Z.; Li, J.; Jiang, Y.; Xu, N.; Li, W.; Zhu, B.; Zhu, J. Spider-Silk-Inspired Nanocomposite Polymers for Durable Daytime Radiative Cooling. *Adv. Mater.* **2022**, *34* (51), 2208236.

(29) Zhong, S.; Zhang, J.; Yuan, S.; Xu, T.; Zhang, X.; Xu, L.; Zuo, T.; Cai, Y.; Yi, L. Self-Assembling Hierarchical Flexible Cellulose Films Assisted by Electrostatic Field for Passive Daytime Radiative Cooling. *Chem. Eng. J.* **2023**, *451*, 138558.

(30) Zeng, S.; Pian, S.; Su, M.; Wang, Z.; Wu, M.; Liu, X.; Chen, M.; Xiang, Y.; Wu, J.; Zhang, M.; Cen, Q.; Tang, Y.; Zhou, X.; Huang, Z.; Wang, R.; Tunuhe, A.; Sun, X.; Xia, Z.; Tian, M.; Chen, M.; Ma, X.; Yang, L.; Zhou, J.; Zhou, H.; Yang, Q.; Li, X.; Ma, Y.; Tao, G. Hierarchical-Morphology Metafabric for Scalable Passive Daytime Radiative Cooling. *Science* **2021**, *373* (6555), 692−696.

(31) Tian, Q.; Tu, X.; Yang, L.; Liu, H.; Zhou, Y.; Xing, Y.; Chen, Z.; Fan, S.; Evans, J.; He, S. Super-Large-Scale Hierarchically Porous Films Based on Self-Assembled Eye-Like Air Pores for High-Performance Daytime Radiative Cooling. *Small* **2022**, *18* (51), 2205091.

(32) Zhang, X.; Yang, W.; Shao, Z.; Li, Y.; Su, Y.; Zhang, Q.; Hou, C.; Wang, H. A Moisture-Wicking Passive Radiative Cooling Hierarchical Metafabric. *ACS Nano* **2022**, *16* (2), 2188−2197.

(33) Wang, H.-D.; Xue, C.-H.; Guo, X.-J.; Liu, B.-Y.; Ji, Z.-Y.; Huang, M.-C.; Jia, S.-T. Superhydrophobic Porous Film for Daytime Radiative Cooling. *Appl. Mater. Today* **2021**, *24*, 101100.